Transcription Factor EB Alleviates Endothelial Cell Inflammation Through NLRP3 Inflammasome-Mediated Cell Pyroptosis in Atherosclerosis

Fengxia Guo (865932892@qq.com)
Department of Clinical Laboratory https://orcid.org/0000-0002-0021-0724
Bing Hu
Department of Clinical Laboratory
Yanhua Sha
Department of Laboratory Medicine
Kangning Zhu
Department of Clinical Laboratory
Gang Li
Department of Clinical Laboratory

Research

Keywords: TFEB, NLRP3 inflammasome, cell pyroptosis, atherosclerosis

Posted Date: December 31st, 2020

DOI: https://doi.org/10.21203/rs.3.rs-132711/v1

Abstract

Background

Increasing evidence suggests that transcription factor EB (TFEB) inhibits inflammation in endothelial cell (ECs) and reduces development of atherosclerosis. However, little is known about the mechanism of action of TFEB on inflammation in atherosclerosis (AS).

Methods

The levels of TFEB, NLRP3, VCAM-1, ICAM-1, E-selectin, MCP-1, cleaved caspase-1, IL-1β and IL-18 in ECs were examined by immunoblotting, quantitative real time-polymerase chain reaction (qRT-PCR) , Enzyme-linked immunosorbent assay. The LDH activity were examined by LDH assay. TUNEL-positive cell were examined by TUNEL assay. The relationship between TFEB and NLRP3 were examined by immunofluorescence and coimmunoprecipitation. The effects of TFEB on atherosclerotic lesions by hematoxylin and eosin, TUNEL and collagen staining in the aortic valve of $ApoE^{-/-}$ mice fed a high fat diet (HFD).

Results

Here, we report that H_2O_2-induced cell pyroptosis and inflammatory response were mainly due to nucleotide-binding oligomerization domain-like receptor protein 3 (NLRP3) inflammasome activation. The nuclear protein TFEB was significantly increased by H_2O_2, and knockdown of TFEB aggravated cell pyroptosis and inflammatory response. TFEB directly bound to NLRP3 and blocked NLRP3-mediated cell pyroptosis and inflammatory response. The effect of H_2O_2 on TFEB might be associated with AMP-activated protein kinase/mechanistic target of rapamycin-dependent signaling pathways.

Conclusions

Our findings indicated that a novel TFEB–NLRP3 axis was a critical regulator in EC pyroptosis and inflammation, which could be potential therapeutic targets in AS and related cardiovascular diseases.

Introduction

It has been shown that oxidative modification of lipids and proteins is detectable in the vascular lesions of atherosclerosis (AS) and the degree of oxidation correlates closely with the severity of the AS [1]. Oxidative-stress-induced injury of endothelial cells (ECs) is one of the main factors in AS, which stimulates the secretion of inflammatory factors and triggers the accumulation of inflammatory factors in ECs, leading to the formation of atherosclerotic plaques [2-5]. Many studies have revealed that antioxidants possess therapeutic benefits to combat the progression of cardiovascular disease [6]. Therefore, reducing oxidative-stress-induced inflammation may be beneficial in preventing the progression of atherosclerosis.

Pyroptosis, also known as inflammatory cell death, is a form of programmed cellular necrosis in which cells continue to swell until the cell membrane ruptures, resulting in the release of cellular contents and activation of a severe inflammatory response. Studies have indicated that pyroptosis plays a key role in the pathogenesis of cardiovascular disease. More importantly, it was found that NLRP3-related downstream signaling molecules (apoptosis-associated speck-like protein containing a CARD [ASC], caspase-1, interleukin [IL]-1β and IL-18) were significantly more expressed in atherosclerotic plaque than in non-atherosclerotic vessels, and higher expression of caspase-1, IL-1β and IL-18 was closely correlated with atherosclerotic plaque fragility, suggesting that activation of the NLRP3 inflammasome mediated the evolution of atherosclerotic lesions [7]. The development of cell pyroptosis is closely related to activation of the NLRP3 inflammasome, which is one of the major inflammatory complexes in cell death. Therefore, research on the therapeutic targets of NLRP3 inflammatory corpuscles and pyroptosis is important for the prevention and treatment of cardiovascular diseases [8]. However, the exact mechanism of action of pyroptosis on AS is still unclear.

Transcription factor EB (TFEB) is a member of the microphthalmia/transcription factor E (MiT/TFE) family of basic helix-loop-helix leucine zipper transcription factors. TFEB is involved in the development of neurodegenerative diseases, cancer and atherosclerotic diseases. TFEB is the master regulator governing gene regulation of autophagy and lysosomal biogenesis, and is involved in many pathophysiological processes, such as mitochondrial function, lipid and energy metabolism, and inflammation [9,10]. Additionally, knockdown of TFEB leads to accumulation of lipid droplets and impairment of lipid degradation [11]. Recently, increased evidence has indicated that TFEB acts as protective factor in AS through inhibition of EC inflammation [9, 12]. Whether TFEB is involved in AS, and its mechanism of action on cell pyroptosis remain to be clarified.

Here, our novel finding confirmed that TFEB inhibited cell pyroptosis induced by NLRP3, which attenuated the H_2O_2-induced inflammatory response in ECs. The mechanism of H_2O_2 regulation of TFEB was mainly due to the mechanistic target of rapamycin (mTOR)-dependent signaling pathways. We explored the role of TFEB and its mechanisms in mediating the NLRP3 inflammasome and cell pyroptosis in the pathogenesis of AS.

Results

Oxidative stress triggers pyroptosis and inflammatory response in ECs.

H_2O_2 can induce an inflammatory response though triggering oxidative stress in cardiovascular disease [13,14]. Recent studies have shown that pyroptosis plays key roles in the inflammatory response. Therefore, we assessed the relationship between H_2O_2 and cell pyroptosis and inflammatory response in ECs. In ECs, H_2O_2 exposure (0, 25, 50 or 100 μmol) increased the inflammatory response as indicated by a dose dependent increase of vascular cell adhesion molecule (VCAM)-1, intercellular adhesion molecule (ICAM)-1, E-selectin and monocyte chemoattractant protein (MCP)-1 expression and production (Figure

1A–C). These results showed that H_2O_2 induced an inflammatory response in ECs. We investigated the effect of H_2O_2 on cell pyroptosis. In ECs exposed to H_2O_2, the level of cleaved caspase-1, IL-1β and IL-18 was significantly increased in a dose-dependent manner (Figure 1D and E), which was accompanied by an increase in lactate dehydrogenase (LDH) activity (Figure 1F). This suggested that H_2O_2 promoted cell pyroptosis. Collectively, our results revealed that H_2O_2-induced cell pyroptosis may contribute to the inflammatory response in ECs.

NLRP3 inflammasome contributes to cell pyroptosis under oxidative stress in ECs.

Many studies have shown that the biochemical function of the NLRP3 inflammasome is to activate caspase-1, which leads to maturation of IL-1β and IL-18 and induction of cell pyroptosis [15]. Thus, we explored a possible effect of H_2O_2 on NLRP3-inflammasome-induced pyroptosis in ECs. H_2O_2 exposure increased expression of NLRP3 (Figure 2A and B). We silenced expression of NLRP3 and investigated its impact on inflammatory response and cell pyroptosis. Knockdown of NLRP3 (Figure S1A) markedly reduced expression and production of VCAM-1, ICAM-1, E-selectin and MCP-1 in ECs (Figure 2C–E). Knockdown of NLRP3 inhibited expression of cleaved caspase-1, IL-1β and IL-18 (Figure 2F and G), along with decreased LDH activity (Figure 2H) and TUNEL-positive ECs (Figure 2I). We investigated the functional role of NLRP3 in pyroptosis and inflammatory response under oxidative stress in ECs. Knockdown of NLRP3 reduced the H_2O_2-induced decrease in production of VCAM-1, ICAM-1, E-selectin and MCP-1 (Figure 2J–L) in ECs. Knockdown of NLRP3 attenuated H_2O_2-induced upregulation of cleaved caspase-1, IL-1β and IL-18 (Figure 2M and N) and LDH activity (Figure 2O). The TUNEL-positive cells induced by H_2O_2 were also enhanced by pcDNA-NLRP3 (overexpression of NLRP3 (Figure S1 B)), suggesting that NLRP3 aggravated cell pyroptosis and inflammatory response induced by H_2O_2 (Figure 2P). These results indicated that NLRP3 contributed to cell pyroptosis by releasing proinflammatory cytokines under oxidative stress.

TFEB is required for pyroptosis and inflammatory response induced by NLRP3 under oxidative stress in ECs.

TFEB in ECs inhibits inflammation and reduces AS development[16]. To further elucidate the essential role of TFEB in regulating pyroptosis and inflammatory response in ECs, we used siRNA to inhibit expression of TFEB (Figure S1C). TFEB knockdown significantly enhanced expression and production of VCAM-1, ICAM-1, E-selectin and MCP-1 (Figure 3A–C), suggesting that TFEB inhibited the inflammatory response. TFEB-shRNA significantly enhanced NLRP3, cleaved caspase-1, IL-1β and IL-18 (Figure 3D and E) expression, along with LDH activity (Figure 3F) and TUNEL-positive cells (Figure 3G). Overexpression of TFEB (Figure S1D) significantly attenuated NLRP3, cleaved caspase-1, IL-1β and IL-18 expression (Figure 3H and I) and LDH activity (Figure 3J). These results indicated that TFEB alleviated cell pyroptosis and inflammatory response. We investigated whether NLRP3 involvement in pyroptosis and the inflammatory response was inhibited by TFEB. Knockdown of NLRP3 attenuated TFEB-shRNA-induced expression and production of VCAM-1, ICAM-1, E-selectin and MCP-1 (Figure 3K–M). Subsequently, knockdown of NLRP3

attenuated TFEB-shRNA-induced expression of cleaved caspase-1, IL-1β and IL-18 in ECs (Figure 3N and O). NLRP3-shRNA treatment decreased TFEB-shRNA-induced LDH activity (Figure 3P), and TFEB-shRNA-induced TUNEL-positive cells were further increased by pcDNA-NLRP3 (Figure 3Q). The results confirmed that TFEB alleviation or pyroptosis and the inflammatory response were mainly due to NLRP3 inhibition in ECs. We elucidated the possible role of TFEB in H_2O_2-induced pyroptosis and inflammatory response in ECs. Cytoplasmic TFEB was markedly decreased and nuclear TFEB was increased by H_2O_2 in a dose-dependent manner (Figure 3R). Overexpression of TFEB markedly suppressed H_2O_2-induced VCAM-1, ICAM-1, E-selectin and MCP-1 level and production (Figure 3S–U), suggesting that TFEB alleviated the inflammatory response induced by H_2O_2 in ECs. Overexpression of TFEB inhibited H_2O_2-induced expression of NLRP3, cleaved caspase-1, IL-1β and IL-18 (Figure 3V and W). In accordance with reverse transcription polymerase chain reaction (RT-PCR) and immunoblotting results, LDH activity induced by H_2O_2 was decreased by pcDNA-TFEB (Figure 3X). The number of TUNEL-positive cells induced by H_2O_2 was also further increased by TFEB-shRNA (Figure 3Y). These results indicated that TFEB suppressed NLRP3 inflammasome expression, which alleviated cell pyroptosis and inflammatory response induced by oxidative stress, suggesting that TFEB exerted a potent protective effect on ECs in the presence of oxidative stress.

TFEB interacts with NLRP3

The above results demonstrated that nuclear translocation of TFEB increased under oxidative stress and TFEB alleviated the NLRP3 levels in ECs. To establish the mechanism of action of TFEB on NLRP3 in AS, we measured colocalization of TFEB and NLRP3 in the presence of H_2O_2, using immunofluorescence confocal microscopy. Colocalization of TFEB and NLRP3 was detected in ECs when exposed to H_2O_2 (Figure 4A). We carried out coimmunoprecipitation using an anti-NLRP3 antibody, followed by western blotting of the expression of TFEB and NLRP3. We demonstrated the presence of TFEB and NLRP3 in the immunoprecipitation group compared with the IgG group, confirming an interaction between TFEB and NLRP3 (Figure 4B). The analysis showed that TFEB interacts with NLRP3.

AMP-activated protein kinase (AMPK)/mTOR signaling pathway contributes to TFEB-mediated cell pyroptosis and inflammatory response under oxidative stress.

The above results confirmed that TFEB inhibited NLRP3 inflammasome activation and cell pyroptosis. A recent study showed that the AMPK/mTOR pathway serves as a novel regulator of cell fate during differentiation via TFEB-dependent regulation of autophagic flux [17,18]. We investigated whether this was also the case in H_2O_2-induced pyroptosis. Phosphorylation of AMPK was increased, whereas phosphorylation of mTOR was decreased by H_2O_2 in a dose-dependent manner, with no change in AMPK and mTOR total protein expression levels (Figure 5A). However, AMPK phosphorylation was decreased and mTOR phosphorylation was increased after AMPK inhibition (Compound C; CC) (Figure.S1E). H_2O_2-induced production of VCAM-1, ICAM-1, E-selectin and MCP-1 was suppressed by CC (Figure 5B–D). H_2O_2-induced NLRP3, cleaved caspase-1, IL-1β and IL-18 protein and mRNA levels were inhibited by CC

(Figure 5E and F) along with LDH activity (Figure 5G) and number of TUNEL-positive cells (Figure 5H). We also found that H_2O_2-induced TFEB nuclear protein was inhibited by CC (Figure 5I). Conversely, cytoplasmic TFEB inhibition by H_2O_2 was reversed by CC, suggesting that the level of TFEB was regulated by H_2O_2 partly through the AMPK/mTOR signaling pathway. These results suggested that H_2O_2 regulated the TFEB expression partly through the mTOR-dependent signaling pathway in ECs.

TFEB alleviates atherosclerotic lesion formation.

To investigate whether TFEB plays a role in the pathogenesis of AS, we explored the effects of TFEB on atherosclerotic lesions by hematoxylin and eosin staining in the aortic valve of $ApoE^{-/-}$ mice fed a high fat diet (HFD). Expression of TFEB in the HFD group was decreased, whereas NLRP3 expression was increased (Figure 6A). TFEB-shRNA induced cell death in $ApoE^{-/-}$ mice treated with HFD (Figure 6B). As expected, the lesion areas and collagen content in the aortic valve were increased in the HFD group, and TFEB-shRNA aggravated the changes in lesion areas and collagen content caused by HFD (Figure 6C). The above findings indicated a protective role of TFEB against the development of vulnerable atherosclerotic plaques.

Discussion

Evidence from experimental and clinical studies have shown that oxidative stress stimulates the formation of atherosclerotic plaques and increases the risk of AS [19,20]. Pyroptosis is a form of lytic programmed cell death, which detects cell swelling, resulting in the release of proinflammatory cytokines (IL-1β and IL-18) [21]. Tu et al. revealed that mild hypothermia alleviates ischemic injury via inhibiting pyroptosis [22]. Zi et al. showed that sirtuin (SIRT)6 attenuated triggering receptor expressed on myeloid cells-1 (TREM)-1-mediated pyroptosis and EC inflammation in acute myocardial infarction [23]. In agreement with previous study, our results showed that the inflammatory response was increased by H_2O_2, and H_2O_2 induced the activation of pyroptosis in ECs. Our results also showed that the inflammatory response induced by H_2O_2 was mainly due to the activation of cell pyroptosis, indicating that H_2O_2-induced pyroptosis might be a cellular mechanism for the inflammatory response in AS. Therefore, the underlying molecular mechanism of oxidative stress in inflammation, except pyroptosis, requires further exploration.

The current study demonstrated that the NLRP3 inflammasome was closely related to cell pyroptosis and plays a crucial role in cardiovascular disease. Numerous studies have shown that components of the NLRP3 inflammasome signaling pathway (NLRP3, ASC, caspase-1, IL-1β and IL-18) are predominantly localized in human carotid unstable atherosclerotic plaques [24]. In the mouse myocarditis model, 1,25-dihydroxyvitamin D3 can inhibit the cardiomyocyte pyroptosis signaling pathway and prevent cardiomyocyte death, and then improve the lesions of myocarditis [25]. The miRNA-9 acts on the protein ELAV-like protein 1, which in turn inhibits expression of caspase-1 and IL-1β in cardiomyocytes, and inhibits high glucose-induced cardiomyocytes pyroptosis[26]. Activation of NLRP3-inflammasome-

regulated pyroptosis can aggravate myocardial ischemic injury [27]. We found that oxidative-stress-mediated NLRP3 inflammasomes play an important role in the development of AS. Moreover, expression of NLRP3 was upregulated by H_2O_2, and H_2O_2 aggravated cell pyroptosis and the inflammatory response. NLRP3 enhanced cell pyroptosis and the inflammatory response induced by H_2O_2. A previous study has revealed that lipopolysaccharide can aggravate hypoxia/reoxygenation and high glucose-induced cardiomyocyte injury by activating reactive oxygen species (ROS)-dependent NLRP3-mediated pyroptosis[28]. Nicotine promotes the development of AS through ROS/NLRP3-regulated EC pyroptosis [29]. These results indicated that oxidative stress triggered NLRP3-induced cell pyroptosis, resulting in an inflammatory response and cell damage, but the exact mechanism of action of oxidative stress in cell pyroptosis needs further investigation.

TFEB is a master regulator of lysosome biogenesis and autophagy. TFEB overexpression acts against AS by reducing production of the proinflammatory cytokine IL-1β and enhancing cholesterol efflux in macrophages. Numerous studies have shown that the disaccharide trehalose acts as a novel inducer of TFEB with similar atheroprotective effects [30]. TFEB has a transcriptional regulatory function during lipid catabolism though proliferator-activated receptor γ coactivator-1α. TFEB represents a novel resveratrol target related to the protection against EC oxidative damage [31]. In agreement with a previous study, we found that TFEB alleviated the inflammatory response in ECs. TFEB also attenuated NLRP3-dependent cell pyroptosis and inflammatory response. These effects of TFEB were further reversed by NLRP3. Nuclear TFEB was upregulated by H_2O_2 and alleviated cell pyroptosis and inflammatory response. Previous studies have shown that overexpression of TFEB suppresses endothelial inflammation and attenuates AS in mice [32]. Collectively, these results indicate that TFEB protects cells from oxidative stress damage. Consistently, in our study, the lesion area was further enhanced in ApoE$^{-/-}$ mice fed an HFD by knockdown of TFEB. The above results provided evidence for the underlying mechanisms of the anti-inflammatory effects of TFEB, in which inhibition of NLRP3-induced pyroptosis may play a key role. However, trehalose activates autophagy and inhibits the activity of the inflammasome via TFEB, and ultimately alleviates the development of AS [30]. Jiang et al. showed that acrolein inhibits EC migration by inducing NLRP3-regulated pyroptosis through ROS-dependent autophagy [33]. The detailed mechanisms of TFEB in pyroptosis by autophagy will be further explored in future studies.

Recent studies have provided evidence that TFEB is regulated by mTOR in the presence of nutrients [34]. The mTOR-dependent pathway is a pivotal mechanism to strengthen the function of TFEB. The phosphorylates and nuclear fraction of TFEB are increased by extracellular signal-regulated kinase 2 [35,36]. The deacetylation effect of SIRT1 and the AMPK/SIRT1 pathway play a critical role in TFEB-regulated gene transcription [37]. We found that H_2O_2-regulated TFEB expression was mainly due to the mTOR-dependent signaling pathway. Moreover, the TFEB/NLRP3 pathway was associated with mTOR-dependent signaling pathways regulated by H_2O_2, which verified the involvement of these pathways in pyroptosis. The detailed mechanisms of action of H_2O_2 in TFEB will be further explored in future studies.

As shown in the schematic diagram in Figure 7, our results provided evidence that TFEB suppressed NLRP3 inflammasome expression and cell pyroptosis, which alleviated the inflammatory response induced by oxidative stress. Moreover, the TFEB suppressed by H_2O_2 was mainly associated with mTOR-dependent signaling. These novel finding are relevant to enhancing our understanding of the pathogenesis of AS and reveal that TFEB could act as novel potential therapeutic target.

Materials And Methods

Regents

Dulbecco's Modified Eagle's Medium (DMEM) and fetal bovine serum were purchased from Gibco (Grand Island Biological Company (New York, NY, USA). Antibodies against rabbit phospho-AMPKα-T172 (AP0116) and phospho-mTOR-S2448 (AP0409), mTOR (A5520) were obtained from Abclonal (Woburn, MA, USA). Antibodies against rabbit AMPKα1 (YT0215) and E-selectin (YT5745) were purchased from Immunoway (Plano, TX, USA). TFEB (ab270604), NLRP3 (ab263899), caspase-1 (ab207802), IL-1β (ab234437), IL-18 (ab243091), VCAM-1 (ab134047), ICAM-1 (ab109361), and MCP-1 (ab214819) were obtained from Abcam (Cambridge, MA, USA). CC (P5499) was purchased from Selleck Chemicals (Shanghai, China). ACTB(RM2001) and Histone (ab1791) was purchased from Abcam.

Cell culture

Human umbilical vein ECs (ATCC CRL-1730) were purchased from American Type Culture Collection (Manassas, VA, USA. The ECs were seeded in DMEM provided with 10% fetal bovine serum at 37°C with 95% air and 5% CO_2. Cells were grown in 6- or 12-well plates or 60-mm dishes and grown to 70%–80% confluence before use.

Western blotting and immunoprecipitation analysis

Protein lysates were separated by 12.5% SDS-PAGE. The western blots were incubated for 12 h with 1:800-diluted primary antibodies, and then incubated for 2 h at room temperature with secondary antibodies. The chemiluminescence of proteins was used by ECL Plus Western Blot Detection Sy stem (Amersham Biosciences, Foster City, CA, USA). Immunoprecipitation analysis was performed as previously described [38]. EC lysates were precleared by a conjunction of 1 mg control IgG and protein A/G PLUS-agarose beads, and then incubated overnight at 4°C with anti-NLRP3 antibodies, with addition of 25 ml protein A/G PLUS-agarose beads. The resulting immunoprecipitates were dissolved in SDS-PAGE sample buffer for electrophoresis and immunoblot analysis.

Quantitative RT-PCR

Total RNA was extracted using TRIzol reagent (Invitrogen, Carlsbad, CA, USA) and reverse transcribed in cultured cells. Real-time PCR was carried out on the LightCycler 480 II (Roche, Pleasanton, CA, USA) with SYBR Green Dye detection (TaKaRa Bio, Mountain View, CA, USA). GAPDH was used for normalization.

All samples were assayed in triplicate and the data were analyzed using the ΔΔCt method. The primer sequences are listed in Supplementary Table 1.

Recombinant plasmid construction

The full-length TFEB and NLRP3 cDNA plasmid was obtained from OriGene (Rockville, MD, USA). TFEB cDNA was magnified by PCR and subcloned into the pcDNA3.1(+) vector. The correct sequence of the TFEB and NLRP3 cDNA was confirmed by sequencing and named pcDNA-TFEB/NLRP3 in the recombinant plasmid.

The siRNA assay

Control siRNA (negative control), siRNA-TFEB and siRNA-NLRP3 were purchased from Ribo Targets (Guangzhou, China). Control samples for all experimental procedures were processed with a nontargeting control mimic sequence of equal concentration. The efficiency of siRNA protein were verified by western blotting. The sequences of TFEB-shRNA, NLRP3-shRNA and control siRNA are listed in Supplementary Table 2.

LDH

The release of LDH can be used to assess cell pyroptosis [39]. The LDH-cytotoxicity Assay Kit was used to detect LDH release (Nanjing Jiancheng Biology Engineering Institute, Nanjing, Jiangsu, China).

Enzyme-linked immunosorbent assay

The concentrations of VCAM-1, ICAM-1, E-selectin and MCP-1 in EC culture supernatants in human serum samples were measured by ELISA kits. These kits were purchased from Abcam.

TUNEL

TUNEL assays for cell and tissue sections were performed using an In Situ Cell Death Detection Kit, POD (Roche, Mannheim, Germany). Nuclei were counterstained with 1.0 μg/mL 4',6-diamidino-2-pheny-indole (DAPI; Beyotime, China) for 6 min to mark the nuclei and detected under a fluorescence microscope (IX81; Olympus, Japan) after TUNEL reaction. Only TUNEL-positive cells that colocalized with DAPI-stained nuclei were counted as positive.

Immunofluorescence

The culture medium was exchanged with fresh medium, and the cells were incubated for 24 h and detected with a confocal laser scanning microscope (LSM 880 with Airyscan; Zeiss, Dublin, CA, USA). The nuclei were stained with DAPI for 15 min. The cells were imaged under a laser scanning confocal microscope (FV300; Olympus).

Animals

ApoE$^{-/-}$ mice with a C57BL/6 background were purchased from the Laboratory Animal Center of Peking University (Beijing, China). To verify the effect of TFEB on AS, male (aged 6 weeks) ApoE$^{-/-}$ mice were randomized into three groups of 10 (ND, HFD, and HFD+TFEB-shRNA-treated groups). The HFD mice were injected with lentivirus siRNA-TFEB (TFEB-shRNA) through the tail vein. Mice were fed an HFD (24% carbohydrate, 55% fat and 21% protein) for 16 weeks. Mice were anesthetized with inhalation of 2% sodium valproate, and 1.5 mL of blood was removed by cardiac puncture at week 16. The mice were euthanized by cervical dislocation, and tissues were collected for further analyses.

Statistical analysis

Data were analyzed using SPSS version 13.0 (SPSS, Chicago, IL, USA). Data are presented as the mean ± SD or median (interquartile range) unless otherwise indicated. The results were analyzed by one-way analysis of variance or unpaired Student's *t*-tests when continuous variables were normally distributed. A two-tailed P value <0.05 was considered statistically significant.

Declarations

Ethics approval and consent to participate

All procedures with animals were approved by the Animal Care and Use Committee of Henan Provincial People' Hospital and were conducted following the institutional guidelines.

Consent for publication

Not applicable.

Availability of data and materials

The datasets generated/analyzed during the current study are available.

Competing interests

The authors declare that they have no conflict of interest.

Funding

This work was supported by the National Natural Sciences Foundation of China (grant numbers 82002199).

Authors' contributions

Fengxia Guo and Gang Li conceived and supervised the study; Fengxia Guo designed experiments; Fengxia Guo, Bing Hu, Yanhua Sha and Kangning Zhu performed experiments; Fengxia Guo, Bing Hu and

Yanhua Sha analysed data; Fengxia Guo wrote the manuscript; Fengxia Guo and Gang Li made manuscript revisions. All authors read and approved the final manuscript.

Acknowledgements

Not applicable.

Supplemental Material

Supplemental data for this article can be accessed on the publisher's website.

References

[1] Forstermann, U., Xia, N. & Li, H. Roles of Vascular Oxidative Stress and Nitric Oxide in the Pathogenesis of Atherosclerosis. *Circ Res.***120**,713-735(2017).

[2] Tabas, I., Garcia,Cardena, G. & Owens, G.K. Recent insights into the cellular biology of atherosclerosis. *J Cell Biol.***209**,13-22(2015).

[3] Zhang, H. et al. MiR-34a/sirtuin-1/foxo3a is involved in genistein protecting against ox-LDL-induced oxidative damage in HUVECs. *Toxicol Lett.***277**,115-122(2017).

[4] Yu, X. et al. IGF-1 alleviates ox-LDL-induced inflammation via reducing HMGB1 release in HAECs. *Acta Biochim Biophys Sin (Shanghai).* **44**,746-51(2012).

[5] Hussain, T. et al. Oxidative Stress and Inflammation: What Polyphenols Can Do for Us? *Oxid Med Cell Longev.* **2016**,7432797(2016).

[6] Zheng, S.et al. Trimetazidine Protects Against Atherosclerosis by Changing Energy Charge and Oxidative Stress. *Med Sci Monit.***24**,8459-8468(2018).

[7] Paramel, Varghese. G. et al. NLRP3 Inflammasome Expression and Activation in Human Atherosclerosis. *J Am Heart Assoc.***5**,e003031 (2016).

[8] Zeng, C., Wang, R. & Tan, H. Role of Pyroptosis in Cardiovascular Diseases and its Therapeutic Implications. *Int J Biol Sci.***15**,1345-1357(2019).

[9] Lu, H. et al. TFEB inhibits endothelial cell inflammation and reduces atherosclerosis. *Sci Signal.***10**, eaah4214 (2017).

[10] Kim, H. J. et al. Carbon monoxide-induced TFEB nuclear translocation enhances mitophagy/mitochondrial biogenesis in hepatocytes and ameliorates inflammatory liver injury. *Cell Death Dis.***9**,1060(2018).

[11] Settembre, C. et al. TFEB controls cellular lipid metabolism through a starvation-induced autoregulatory loop. *Nat Cell Biol.***15**,647-58(2013).

[12] Song, W. et al. Endothelial TFEB (Transcription Factor EB) Restrains IKK (IkappaB Kinase)-p65 Pathway to Attenuate Vascular Inflammation in Diabetic db/db Mice. *Ar.terioscler Thromb Vasc Biol.***39**,719-30(2019).

[13] Zhang, Q. et al. Folic acid improves abnormal behavior via mitigation of oxidative stress, inflammation, and ferroptosis in the BTBR T+ tf/J mouse model of autism. *J Nutr Biochem.***71**,98-109(2019).

[14] Li, H. et al. Piceatannol alleviates inflammation and oxidative stress via

modulation of the Nrf2/HO-1 and NF-kappaB pathways in diabetic cardiomyopathy.

Chem Biol Interact. **310**,108754(2019).

[15] He, Y., Hara, H. & Nunez, G. Mechanism and Regulation of NLRP3

Inflammasome Activation. *Trends Biochem Sci.***41**,1012-1021(2016).

[16] Brady, O. A., Martina, J.A. & Puertollano, R. Emerging roles for TFEB in the immune response and inflammation. *Autophagy*. **14**,181-189(2018).

[17] Wu, H. et al. Metformin Promotes the Survival of Random-Pattern Skin Flaps by Inducing Autophagy via the AMPK-mTOR-TFEB signaling pathway. *Int J Biol Sci.***15**, 325-340(2019).

[18] Kim, SH. et al. Ezetimibe ameliorates steatohepatitis via AMP activated protein

kinase-TFEB-mediated activation of autophagy and NLRP3 inflammasome inhibition. *Autophagy.***13**,1767-1781(2017).

[19] Garcia, N., Zazueta, C. & Aguilera,Aguirre. L. Oxidative Stress and Infla

mmation in Cardiovascular Disease. *Oxid Med Cell Longev*. **2017**,5853238(2017).

[20] Ito, F., Sono, Y. & Ito ,T. Measurement and Clinical Significance of Lipid

Peroxidation as a Biomarker of Oxidative Stress: Oxidative Stress in Diabetes,

Atherosclerosis, and Chronic Inflammation. *Antioxidants (Basel).* **8,** 72(2019).

[21] Lu, F. et al. Emerging insights into molecular mechanisms underlying pyroptosis

and functions of inflammasomes in diseases. *J Cell Physiol.***235**,3207-3221(2020).

[22] Tu, Y. et al. Mild hypothermia alleviates diabetes aggravated cerebral ischemic injury via activating autophagy and inhibiting pyroptosis. *Brain Res Bull.***150**,1-12(2019).

[23] Zi, Y. et al. Sirt6-induced autophagy restricted TREM-1-mediated pyroptosis in ox-LDL-treated endothelial cells: relevance to prognostication of patients with acute myocardial infarction. *Cell Death Discov.***5**,88(2019).

[24] Jha, J.C., Ho, F., Dan, C. and Jandeleit,Dahm. K. A causal link between oxidative stress and inflammation in cardiovascular and renal complications of diabetes. *Clin Sci (Lond).* **132**,1811-1836(2018).

[25] Liu, N., Su, H., Zhang, Y., Liu, Z. & Kong, J. Cholecalciterol cholesterol emulsion attenuates experimental autoimmune myocarditis in mice via inhibition of the pyroptosis signaling pathway. *Biochem Biophys Res Commun.***493**,422-428(2017).

[26] Jeyabal, P.et al. MicroRNA-9 inhibits hyperglycemia-induced pyroptosis in human ventricular cardiomyocytes by targeting ELAVL1. *Biochem Biophys Res Commun.* **471**,423-9(2016).

[27] Qiu ,Z. et al. NLRP3 Inflammasome Activation-Mediated Pyroptosis Aggravates Myocardial Ischemia/Reperfusion Injury in Diabetic Rats. *Oxid Med Cell Longev.***2017**,9743280(2017).

[28] Qiu, Z.et al. Lipopolysaccharide (LPS) Aggravates High Glucose- and Hypoxia/Reoxygenation-Induced Injury through Activating ROS-Dependent NLRP3 Inflammasome-Mediated Pyroptosis in H9C2 Cardiomyocytes. *J Diabetes Res.***2019**,8151836(2019).

[29] Wu, X. et al. Nicotine promotes atherosclerosis via ROS-NLRP3-mediated endothelial cell pyroptosis. *Cell Death Dis.***9**,171(2018).

[30] Evans, T.D., Jeong, S.J., Zhang, X., Sergin, I. & Razani, B. TFEB and trehalose drive the macrophage autophagy-lysosome system to protect against atherosclerosis. *Autophagy.***14**,724-726(2018).

[31] Zhou, X. et al. Resveratrol attenuates endothelial oxidative injury by inducing autophagy via the activation of transcription factor EB. *Nutr Metab (Lond).***16**,42(2019).

[32] Wang, Y.T. et al. Activation of TFEB ameliorates dedifferentiation of arterial smooth muscle cells and neointima formation in mice with high-fat diet. *Cell Death Dis.***10**,676 (2019).

[33] Jiang, C. et al. Acrolein induces NLRP3 inflammasome-mediated pyroptosis and suppresses migration via ROS-dependent autophagy in vascular endothelial cells. *Toxicology.***410**,26-40(2018).

[34] Napolitano, G. et al. mTOR-dependent phosphorylation controls TFEB nuclear export. *Nat Commun.***9**,3312(2018).

[35] Settembre, C. & Ballabio, A. TFEB regulates autophagy: an integrated

coordination of cellular degradation and recycling processes. *Autophagy.***7**,1379

81(2011).

[36] Settembre, C. et al. A lysosome-to-nucleus signalling mechanism senses and

regulates the lysosome via mTOR and TFEB. *EMBO J.* **31**,1095-108(2012).

[37] Huang, J.et al. Exercise activates lysosomal function in the brain through AMPK-SIRT1-TFEB pathway. *CNS Neurosci Ther.***25**,796-807(2019).

[38] Sun, Y., Hu, G., Zhang, X. & Minshall, R.D. Phosphorylation of caveolin-1 regulates oxidant-induced pulmonary vascular permeability via paracellular and transcellular pathways. *Circ Res.***105**,676-85 (2009).

[39] Wree, A.et al. NLRP3 inflammasome activation results in hepatocyte pyroptosis,

liver inflammation, and fibrosis in mice. *Hepatology.***59**,898-910(2014).

Figures

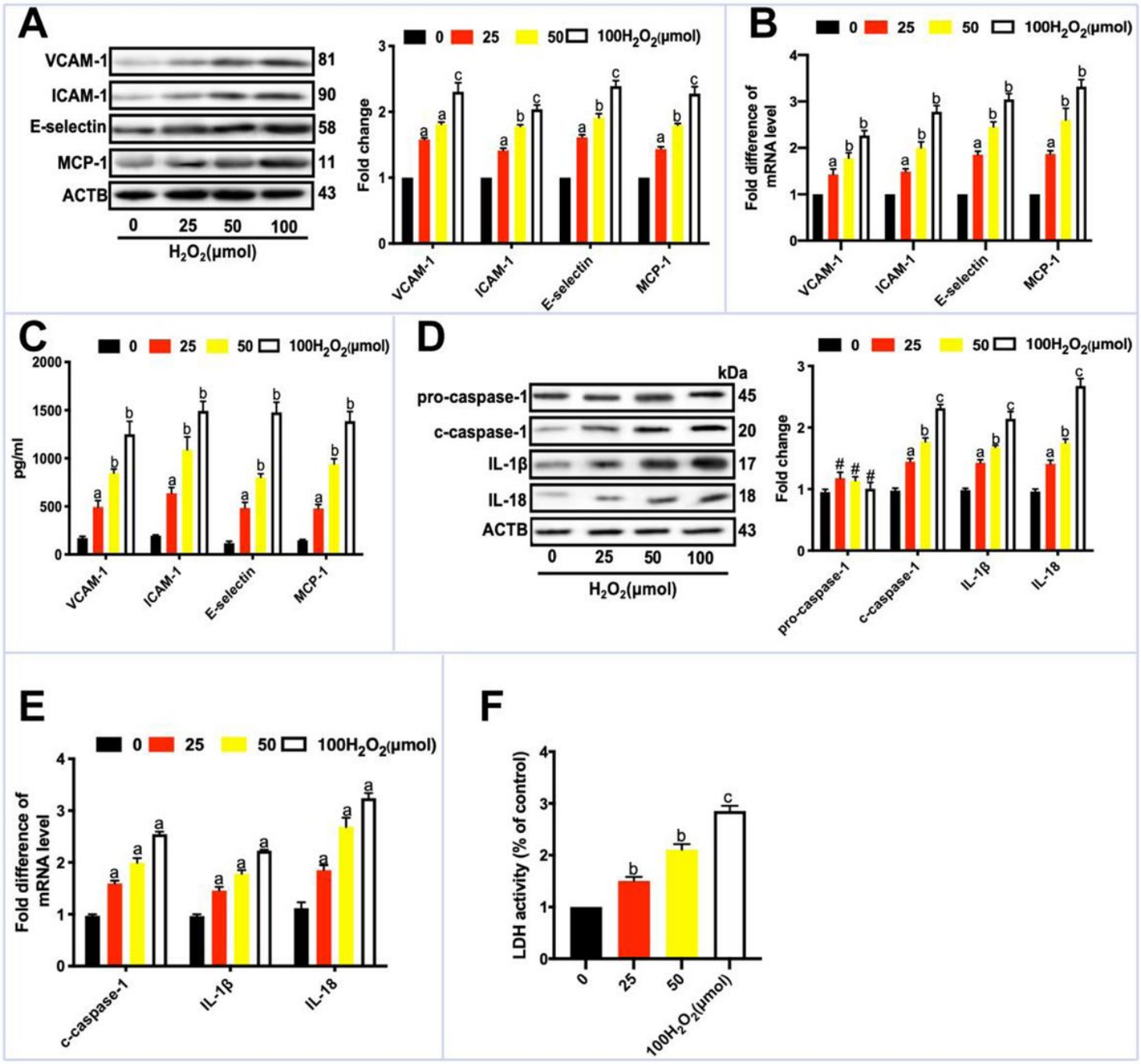

Figure 1

Oxidative stress triggers pyroptosis and inflammatory response in ECs. ECs were treated with H2O2 (0, 25, 50, or 100 μmol) for 24 h. (A) Expression of VCAM-1, ICAM-1, E-selectin and MCP-1 was measured by western blotting. aP<0.05, bP<0.01, and cP<0.001 versus no treatment. (B) Expression of VCAM-1, ICAM-1, E-selectin, and MCP-1 detected by RT-PCR. aP<0.05 and bP<0.01 versus no treatment. (C) Expression of VCAM-1, ICAM-1, E-selectin, and MCP-1 detected by ELISA. aP<0.05 and bP<0.01 versus no treatment. (D) Expression of pro-caspase-1, c-caspase-1, IL-1β, and IL-18 measured by western blotting. aP<0.05, bP<0.01, cP<0.001 and #P<NS versus no treatment. (E) Expression of c-caspase-1, IL-1β, and IL-18

measured by RT-PCR. aP<0.05 versus no treatment. (F) Activity of LDH. bP<0.01 and cP<0.001 versus no treatment. All values are expressed as the mean ± SD (n=3).

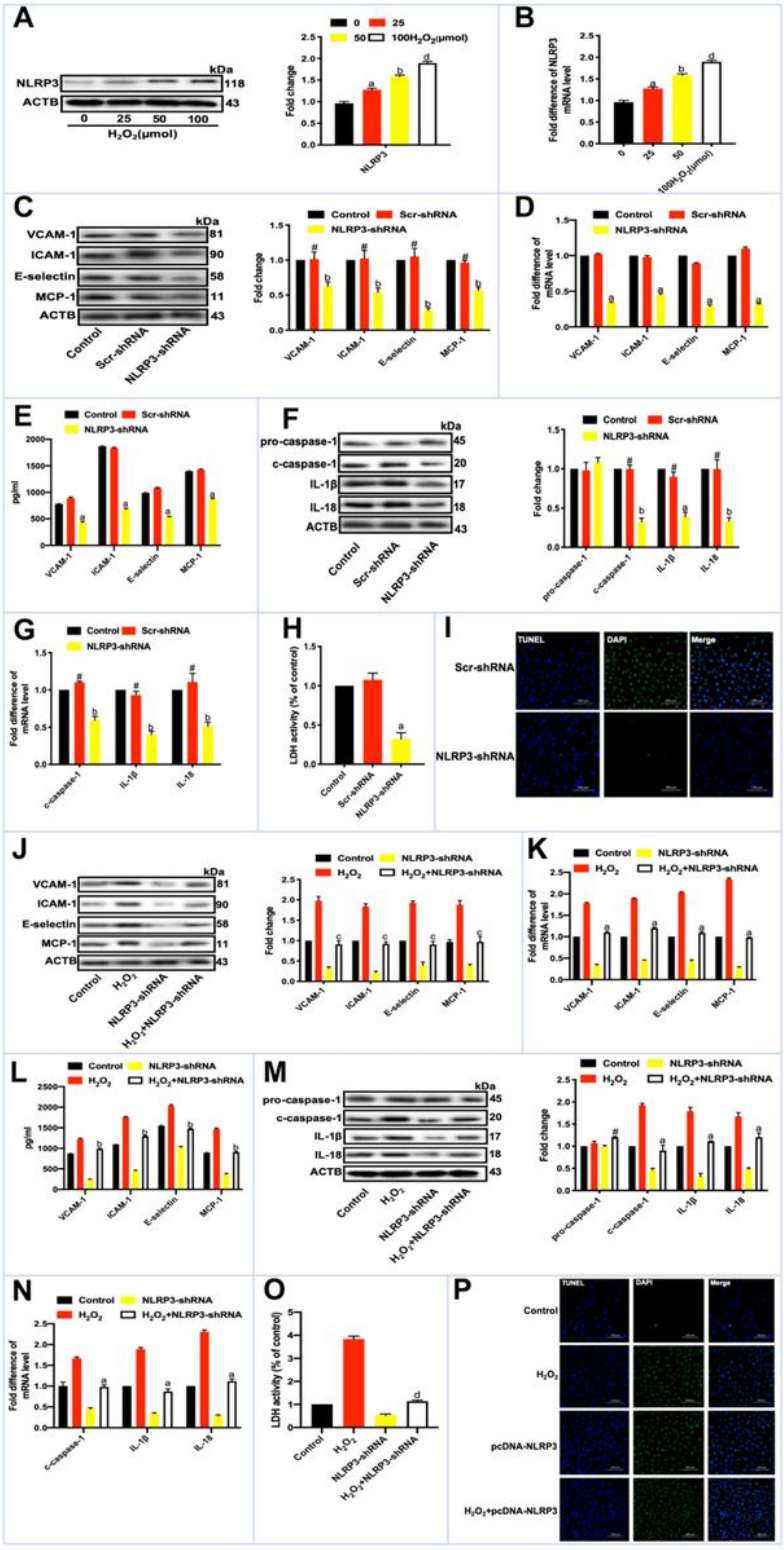

Figure 2

NLRP3 inflammasome contributes to cell pyroptosis under oxidative stress in ECs. (A, B) ECs treated with H2O2 (0, 25, 50, or 100 μmol) for 24 h. (A) Expression of NLRP3 measured by western blotting. aP<0.05, bP<0.01, and dP<0.0001 versus no treatment. (B) Expression of NLRP3 measured by RT-PCR. aP<0.05,

bP<0.01, and dP<0.0001 versus no treatment. (C-H) ECs treated with NLRP3-shRNA or Scr-shRNA. (C) Expression of VCAM-1, ICAM-1, E-selectin, and MCP-1 detected by western blotting. bP<0.01 versus treatment with Scr-shRNA; #P<NS versus treatment with control. (D) Expression of VCAM-1, ICAM-1, E-selectin, and MCP-1 detected by RT-PCR. aP<0.05 versus treatment with Scr-shRNA. (E) Expression of VCAM-1, ICAM-1, E-selectin, and MCP-1 detected by ELISA. aP<0.05 versus treatment with Scr-shRNA. (F) Expression of pro-caspase-1, c-caspase-1, IL-1β, and IL-18 detected by western blotting. aP<0.05 and bP<0.01 versus treatment with Scr-shRNA; #P<NS versus treatment with control. (G) Expression of c-caspase-1, IL-1β, and IL-18 detected by RT-PCR, bP<0.01 versus treatment with Scr-shRNA; #P<NS versus treatment with control. (H) Activity of LDH. aP<0.05 versus treatment with Scr-shRNA. (I) TUNEL (green) double-positive cells were measured in the presence of NLRP3-shRNA. Nuclei stained blue with DAPI. Magnification 200×. Scale bar=100 μm. (J-O) ECs treated with NLRP3-shRNA before H2O2 (100 μmol) for 24 h. (J) Expression of VCAM-1, ICAM-1, E-selectin and MCP-1 detected by western blotting. cP<0.001 versus treatment with H2O2 alone. (K) Expression of VCAM-1, ICAM-1, E-selectin and MCP-1 detected by RT-PCR. aP<0.05 versus treatment with H2O2 alone. (L) Expression of VCAM-1, ICAM-1, E-selectin and MCP-1 detected by ELISA. bP<0.01 versus treatment with H2O2 alone. (M) Expression of pro-caspase-1, caspase-1, IL-1β and IL-18 detected by western blotting. aP<0.05 and #P<NS versus treatment with H2O2 alone. (N) Expression of c-caspase-1, IL-1β and IL-18 detected by RT-PCR. aP<0.05 versus treatment with H2O2 alone. (O) Activity of LDH. dP<0.0001 versus treatment with H2O2. (P) TUNEL (green) double-positive cells measured in the presence of H2O2 and pcDNA-NLRP3. Nuclei stained blue with DAPI. Magnification ×200. Scale bar=100 μm. All values are expressed as the mean ± SD (n=3).

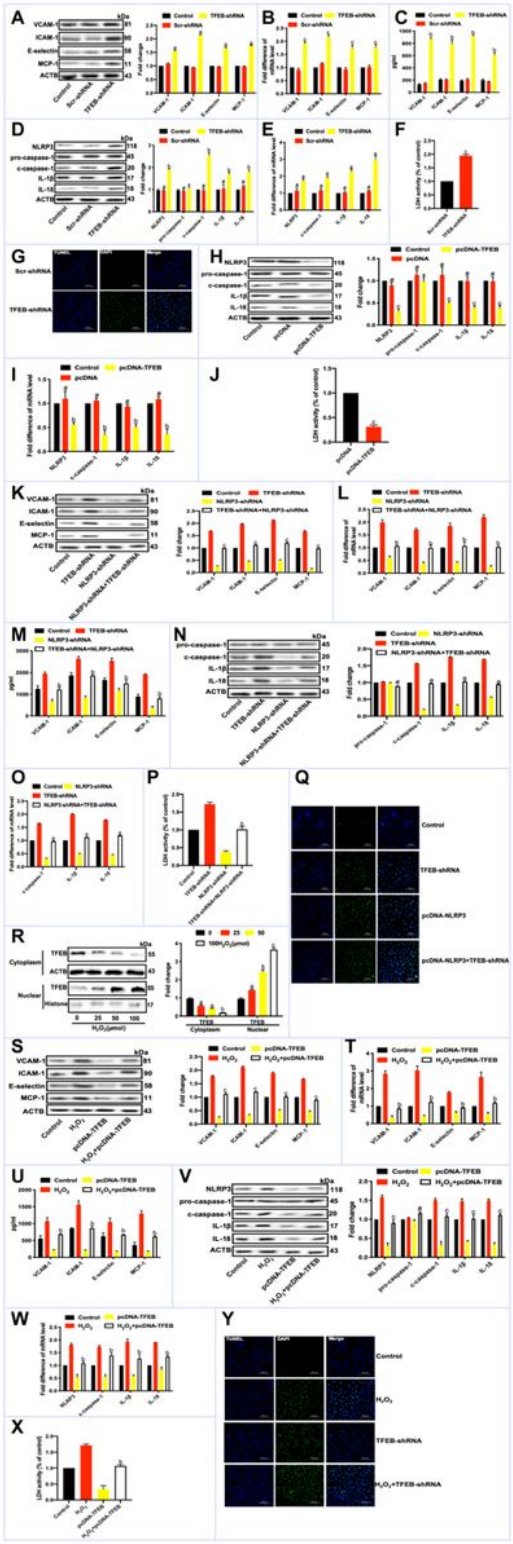

Figure 3

TFEB is required for pyroptosis and inflammatory response induced by NLRP3 under oxidative stress in ECs. (A, B) ECs were treated with TFEB-shRNA or Scr-shRNA. (A) Expression of VCAM-1, ICAM-1, E-selectin and MCP-1 detected by western blotting. aP<0.05 versus treatment with Scr-shRNA. (B) Expression of VCAM-1, ICAM-1, E-selectin and MCP-1 detected by RT-PCR. cP<0.001 versus treatment with Scr-shRNA. (C) ECs were treated with TFEB-shRNA or Scr-RNA. Expression of VCAM-1, ICAM-1, E-selectin and MCP-1

detected by ELISA. bP<0.01 versus treatment with Scr-shRNA. (D–F) ECs treated with TFEB-shRNA and Scr-shRNA for 24 h. (D) Expression of NLRP3, pro-caspase-1, c-caspase-1, IL-1β and IL-18 measured by western blotting. bP<0.01 and *P<NS versus treatment with Scr-shRNA alone; #P<NS versus treatment with control. (E) Expression of NLRP3, c-caspase-1, IL-1β and IL-18 measured by RT-PCR. aP<0.05 versus treatment with Scr-shRNA alone; #P<NS versus treatment with control. (F) Activity of LDH. cP<0.001 versus treatment with Scr-shRNA. (G) TUNEL (green) double-positive cells measured in the presence of TFEB-shRNA and Scr-shRNA. Nuclei were stained blue with DAPI. Magnification 200×. Scale bar=100 μm. (H-J) ECs treated with pcDNA-TFEB or pcDNA. (H) Expression of NLRP3, pro-caspase-1, c-caspase-1, IL-1β and IL-18 detected by western blotting. cP<0.001 and *P<NS versus treatment with pcDNA; #P<NS versus treatment with control . (I) Expression of NLRP3, caspase-1, IL-1β and IL-18 detected by RT-PCR. bP<0.01 versus treatment with pcDNA; #P<NS versus treatment with control. (J) Activity of LDH. cP<0.001 versus treatment with pcDNA. (K-P) ECs treated with NLRP3-shRNA before TFEB-shRNA for 24 h. (K) Expression of VCAM-1, ICAM-1, E-selectin and MCP-1 detected by western blotting. cP<0.001 versus treatment with TFEB-shRNA alone. (L) Expression of VCAM-1, ICAM-1, E-selectin and MCP-1 detected by RT-PCR. bP<0.01 versus treatment with TFEB-shRNA alone. (M) Expression of VCAM-1, ICAM-1, E-selectin and MCP-1 detected by ELISA. bP<0.01 versus treatment with TFEB-shRNA alone. (N) Expression of pro-caspase-1, c-caspase-1, IL-1β and IL-18 detected by western blotting. aP<0.05 and #P<NS versus treatment with TFEB-shRNA alone. (O) Expression of c-caspase-1, IL-1β and IL-18 detected by RT-PCR. aP<0.05 versus treatment with TFEB-shRNA alone. (P) Activity of LDH. bP<0.01 versus treatment with TFEB-shRNA alone. (Q) TUNEL (green) double-positive cells measured in the presence of TFEB-shRNA and pcDNA-NLRP3. Nuclei stained blue with DAPI. Magnification 200×. Scale bar=100 μm. (R–X) ECs treated with H2O2 (0, 25, 50, or 100 μmol) for 24 h. (R) Cytoplasmic and nuclear TFEB measured by western blotting. aP<0.05, bP<0.01 and cP<0.001 versus no treatment. (S) Expression of VCAM-1, ICAM-1, E-selectin and MCP-1 detected by western blotting. cP<0.001 versus treatment with H2O2 alone. (T) Expression of VCAM-1, ICAM-1, E-selectin and MCP-1 detected by RT-PCR. bP<0.01 versus treatment with H2O2 alone. (U) Expression of VCAM-1, ICAM-1, E-selectin and MCP-1 detected by ELISA. bP<0.01 versus treatment with H2O2 alone. (V) Expression of NLRP3, pro-caspase-1, c-caspase-1, IL-1β and IL-18 detected by western blotting. cP<0.001 and #P<NS versus treatment with H2O2 alone. (W) Expression of NLRP3, c-caspase-1, IL-1β and IL-18 detected by RT-PCR. bP<0.01 versus treatment with H2O2 alone. (X) Activity of LDH. bP<0.01 versus treatment with H2O2 alone. (Y) TUNEL (green) double-positive cells measured in the presence of H2O2 (100 μmol) and TFEB-shRNA. Nuclei stained blue with DAPI. Magnification 200×. Scale bar=100 μm. All values are expressed as the mean ± SD (n=3).

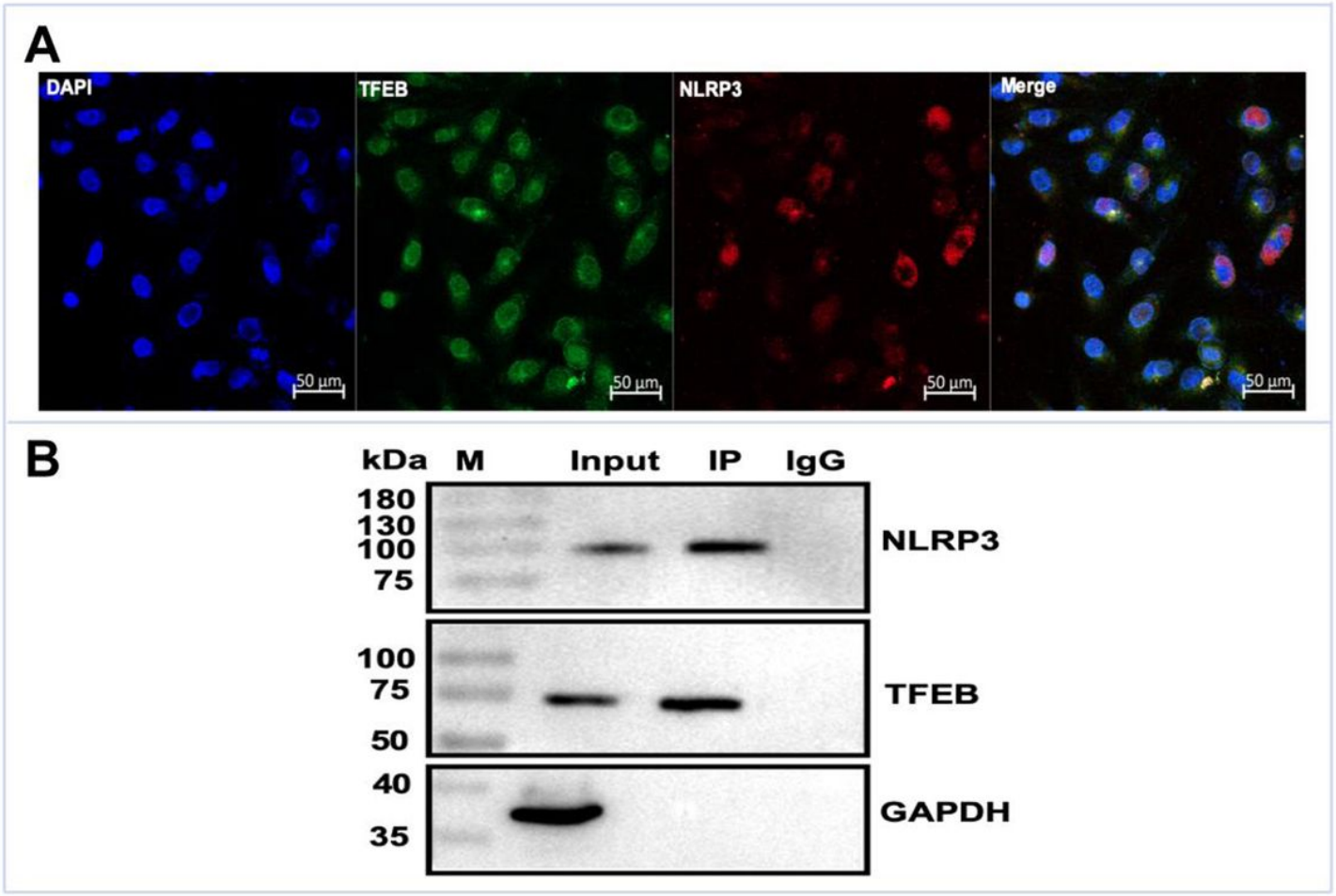

Figure 4

TFEB interacts with NLRP3 (A) H2O2 (100 μmol)-treated ECs stained for TFEB (green) and NLRP3 (red) and analyzed by confocal microscopy. Colocalization of NLRP3 and TFEB was apparent; scale bar: 50 μm. (B) Coimmunoprecipitation of endogenous TFEB with NLRP3. ECs were treated with vehicle or sodium azide for 3 h. Cell lysates subjected to immunoprecipitation using rabbit-anti-TFEB antibody or rabbit IgG. The immunoprecipitates were separated by SDS-PAGE and blotted with TFEB and NLRP3 antibodies.

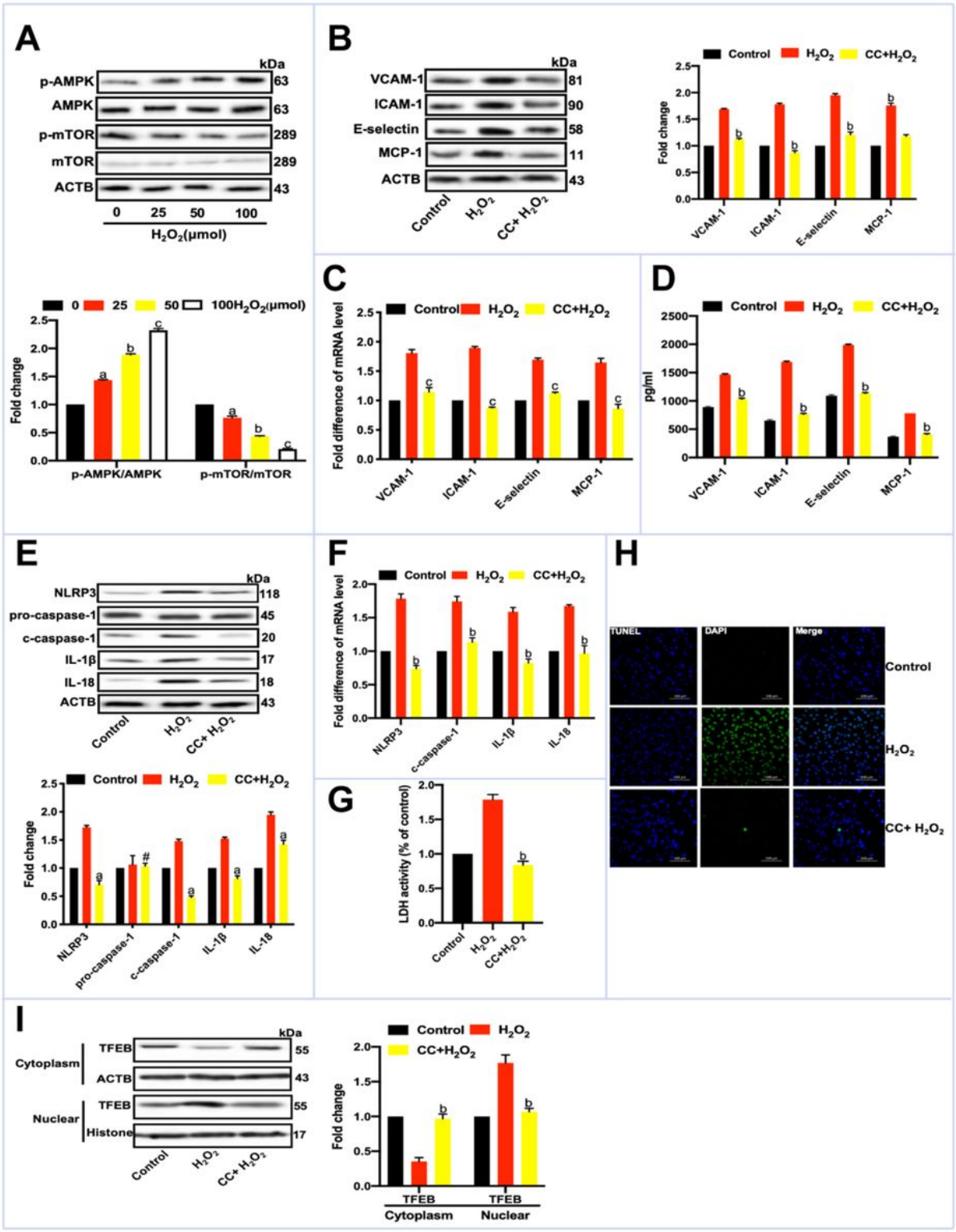

Figure 5

AMP-activated protein kinase (AMPK)/mTOR signaling pathway contributes to TFEB-mediated cell pyroptosis and inflammatory response under oxidative stress. (A) ECs treated with H2O2 (0, 25, 50 or 100 μmol) for 24 h. Total and phosphorylation levels of mTOR and AMPK were determined by western blotting. aP<0.05, bP<0.01 and cP<0.001 versus no treatment. (B-G) ECs treated with AMPK inhibitor (5 μm CC) for 1 h before H2O2 (100 μmol) (B) Expression of VCAM-1, ICAM-1, E-selectin and MCP-1 detected

by western blotting, bP<0.01 versus treatment with H2O2 alone. (C) Expression of VCAM-1, ICAM-1, E-selectin and MCP-1 detected by RT-PCR, cP<0.001 versus treatment with H2O2 alone. (D) Expression of VCAM-1, ICAM-1, E-selectin and MCP-1 detected by ELISA, bP<0.01 versus treatment with H2O2 alone. (E) Expression of NLRP3, pro-caspase-1, c-caspase-1, IL-1β and IL-18 measured by western blotting. aP<0.05 and #P<NS versus treatment with H2O2 alone. (F) Expression of NLRP3, c-caspase-1, IL-1β and IL-18 measured by RT-PCR. bP<0.01 versus treatment with H2O2 alone. (G) Activity of LDH, bP<0.01 versus treatment with H2O2 alone. (H) TUNEL (green) double-positive cells were measured in the presence of H2O2 (100 μmol) and CC. Nuclei stained blue with DAPI. Magnification 200×. Scale bar=100 μm. (I) ECs were treated with CC for 1 h before H2O2 (100 μmol). Cytoplasmic and nuclear levels of TFEB determined by western blotting. bP<0.01 versus treatment with H2O2 alone. All values are expressed as the mean ± SD (n=3).

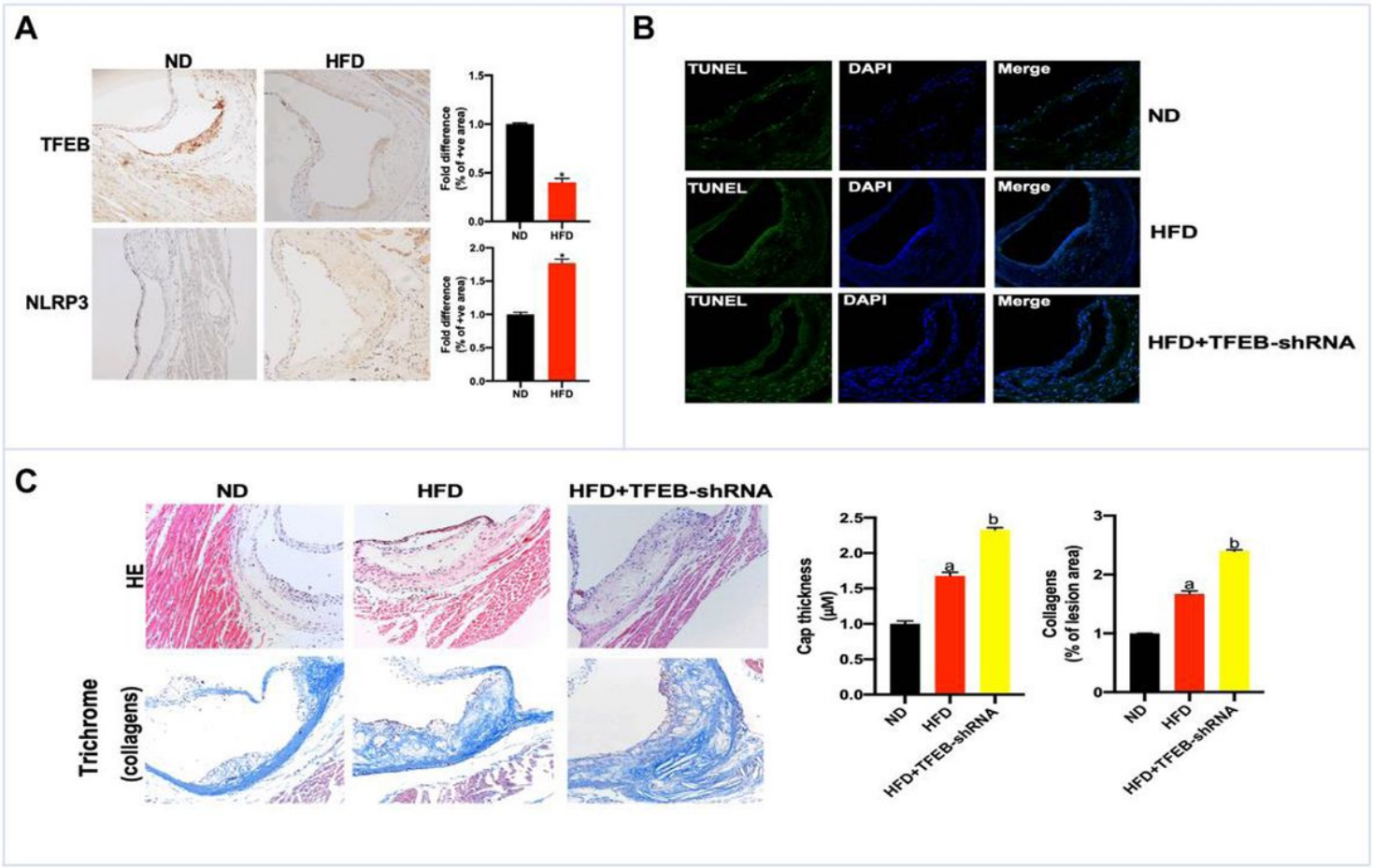

Figure 6

TFEB alleviates atherosclerotic lesion formation. (A) Aorta valve from apoE−/− mice stained by immunohistochemistry for TFEB and NLRP3 in the normal diet (ND) or HFD mice (n=10 mice/group). Magnification 200×, *P<0.05 versus ND group. (B) Number of necroptotic cells (green) in the aorta valve of apoE−/− mice transfected with ND, HFD and HFD+TFEB-shRNA was measured by the TUNEL assay. Nuclei stained blue by DAPI (n=10 mice/group). Magnification 200×. (C) Representative staining of an

aortic valve with HE and trichrome staining in the ND, HFD and HFD+TFEB-shRNA mice group. aP<0.05 versus ND group, bP<0.01 versus HFD group.

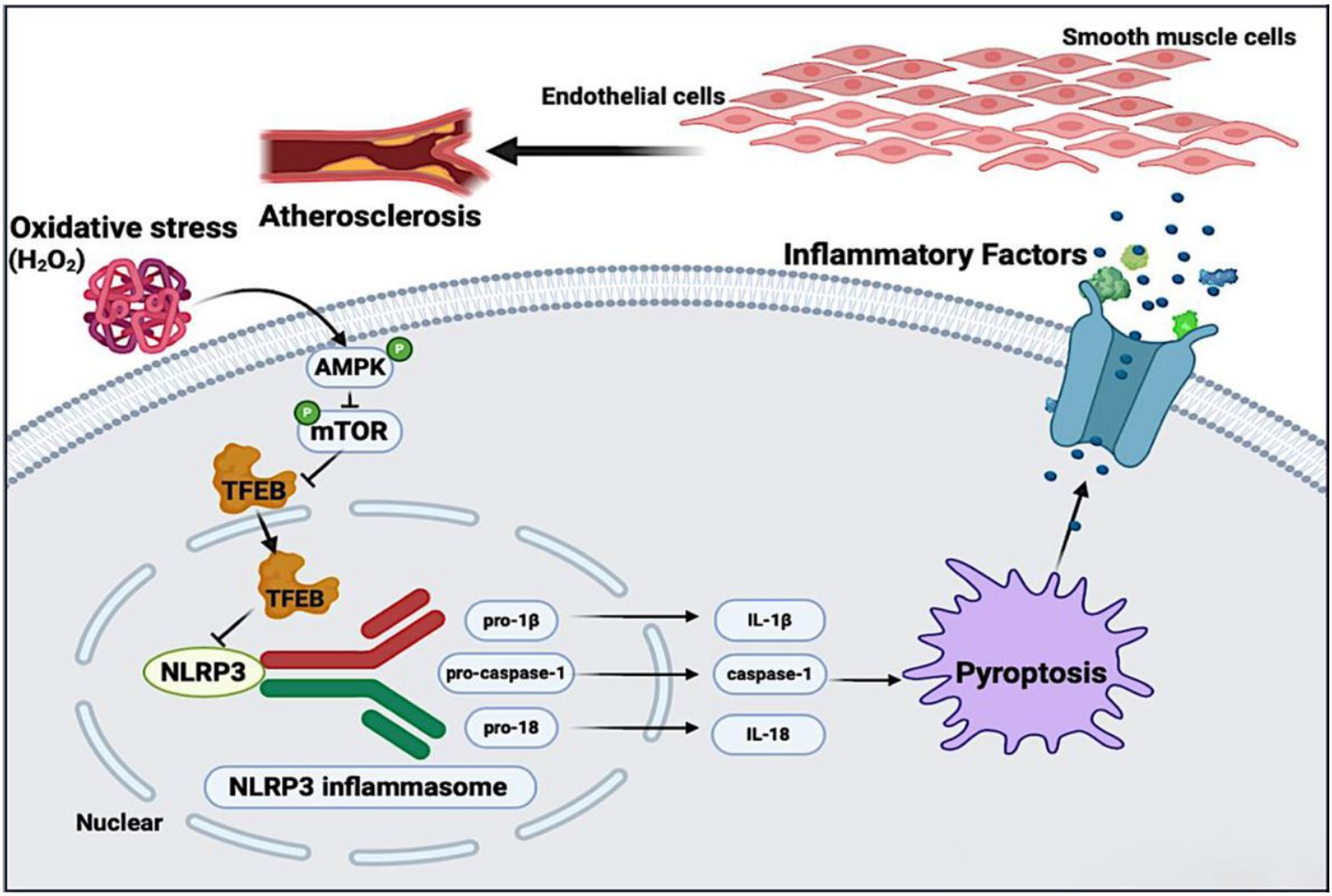

Figure 7

Schematic diagram of the main findings of this study. Our results indicated that TFEB suppressed NLRP3 expression, which alleviated the inflammatory response induced by oxidative stress through inhibition of cell pyroptosis. Moreover, the TFEB increased by H2O2 was associated with mTOR-dependent signaling pathway inactivation.